# Electronic supplementary information (ESI)

**Dynamic Readout of Optical Information Based on The Color-Tunable Emitting Electron-Trapping Material $BaAl_{12}O_{19}$: $Eu^{2+}$ towards High Security Level Optical Data Storage and Anti-Counterfeiting**

Junxiao Wu [a], Lei Zhao [a, d]*, Wenbo Chen [c], Youlin Yang [a], Yifan Wang [a], Xuhui Xu [b]*

[a] *School of Physics and Opto-Electronic Technology, Collaborative Innovation Center of Rare-Earth Optical Functional Materials and Devices Development, Baoji University of Arts and Sciences, Baoji, Shanxi 721016, P. R. China*

[b] *College of Materials Science and Engineering, Kunming University of Science and Technology, Kunming 650093, P. R. China*

[c] *Engineering Research Center of New Energy Storage Devices and Applications, Chongqing University of Arts and Sciences, Chongqing 402160, P. R. China*

[d] *Pillar of Engineering Product Development, Singapore University of Technology and Design, 8 Somapah Road, Singapore 487372, Singapore*

**Corresponding Author's:*

*E-mail: zhaoleibjwl@163.com (Lei Zhao).*

*E-mail: xuxuh07@126.com (Xuhui Xu).*

**Table S1.** Final refined structural parameters for $BaAl_{12}O_{19}$: 7%$Eu^{2+}$

| **Formula** | $BaAl_{12}O_{19}$: $Eu^{2+}$ |
|---|---|
| **Crystal system** | Hexagonal |
| **Space group** | *P 63/mmc* (194) |
| **Vol (Å$^3$)** | 622.47(7) |
| **Unit cell dimens (Å)** | a= b= 5.589(3), c= 22.704(1) |
| **Reliability factors** | $R_{wp}$= 11.02% $R_p$= 9.84% |
| **Program** | GSAS |
| **Profile range** | 5- 80° |
| **Step** | 0.006° |
| **Radiation** | Cu Kα (λ = 1.58184 Å) |

4

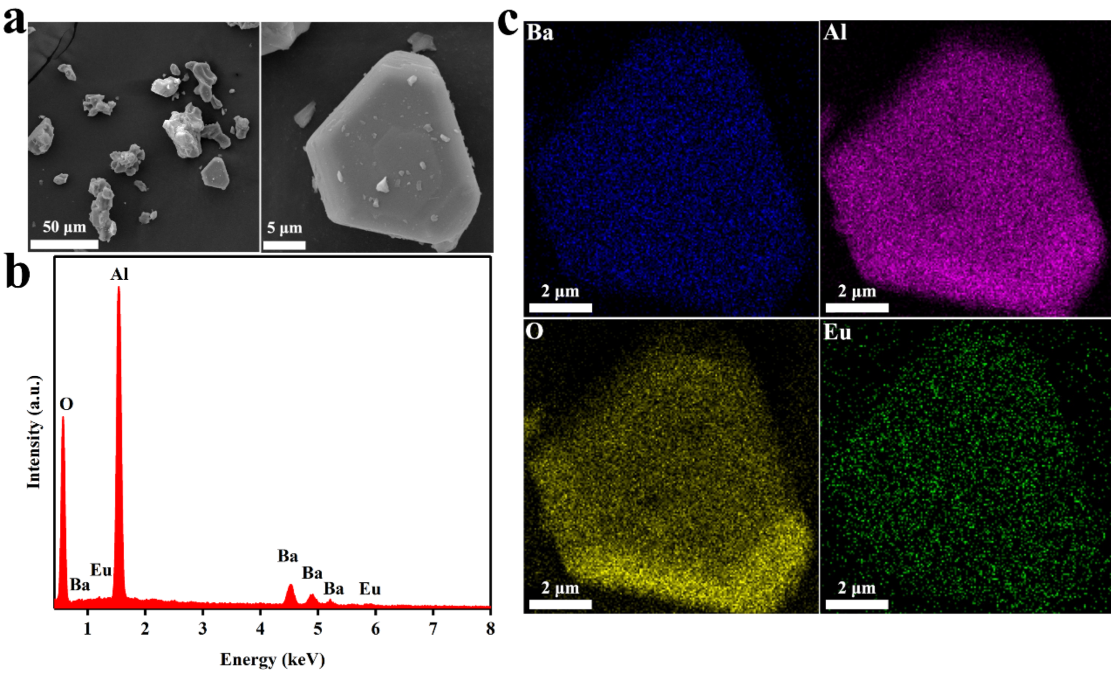


**Figure S1. (a)** SEM images, **(b)** EDS pattern and **(c)** elemental mapping images of Ba, Al, O and Eu for $BaAl_{12}O_{19}$: 7%$Eu^{2+}$.

The SEM image of the $BaAl_{12}O_{19}$: 7%$Eu^{2+}$ sample synthesized under an air atmosphere is shown in **Figure S1(a).** It can be seen that the studied samples exhibit an irregular granular shape. **Figure S1(b)** shows the EDS spectrum. **Figure S1(c)** is the element distribution of Ba, Al, O, and Eu, which shows that the sample contains Ba, Al, Eu, and O elements, and they are uniformly distributed in the entire sample.

**Discussion S1:**

**The self-reduction process:**

The reduction of $Eu^{3+}$ to $Eu^{2+}$ in $BaAl_{12}O_{19}$ in air condition can be explained with the model of the charge compensation mechanism. As $Eu^{3+}$ ions are doped into $BaAl_{12}O_{19}$ , $Eu^{3+}$ ions replace $Ba^{2+}$ ions. To maintain charge balance, two $Eu^{3+}$ ions are needed to substitute for three $Ba^{2+}$ ions. Hence, one vacancy defect $V_{Ba}^{''}$ with two negative charges and two positive defects of $Eu_{Ba}^{\cdot}$ will be created by each substitution of every two $Eu^{3+}$ ions in the compounds. The $V_{Ba}^{''}$ then acts as the donor of electrons, while the two defects become acceptors of electrons. Consequently, by thermal stimulation, the negative charges in vacancy defects of $V_{Ba}^{''}$ will be transferred to $Eu^{3+}$ sites and reduce $Eu^{3+}$ to $Eu^{2+}$. The whole process could be presented in the following equations: [3-5]

$$3Ba^{2+} + 2Eu^{3+} = V_{Ba}^{''} + 2Eu_{Ba}^{\cdot}$$

$$V_{Ba}^{''} = V_{Ba} + 2e$$

$$2Eu_{Ba}^{\cdot} + 2e = 2Eu_{Ba}$$

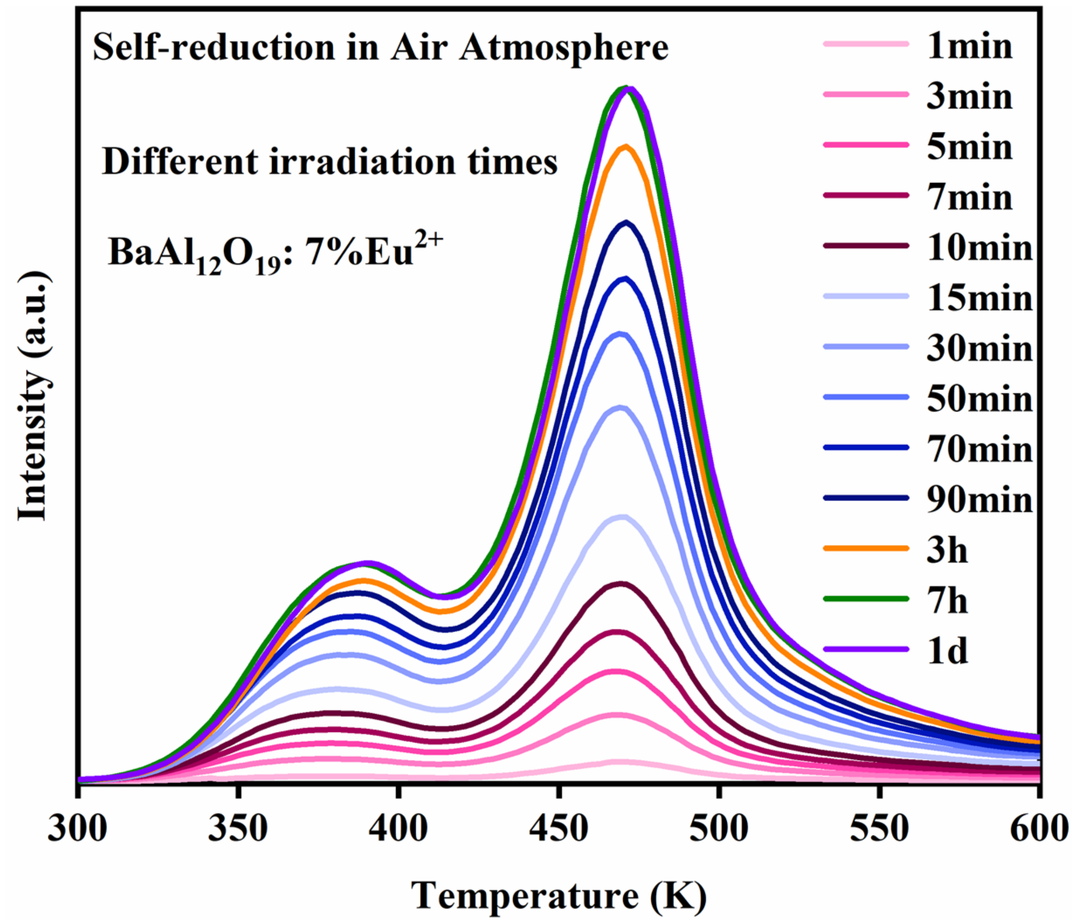


**Figure S2.** TL curves of $BaAl_{12}O_{19}$: 7%$Eu^{2+}$ sample measured after irradiation by UV light at various durations. (Self-reduction in air atmosphere)

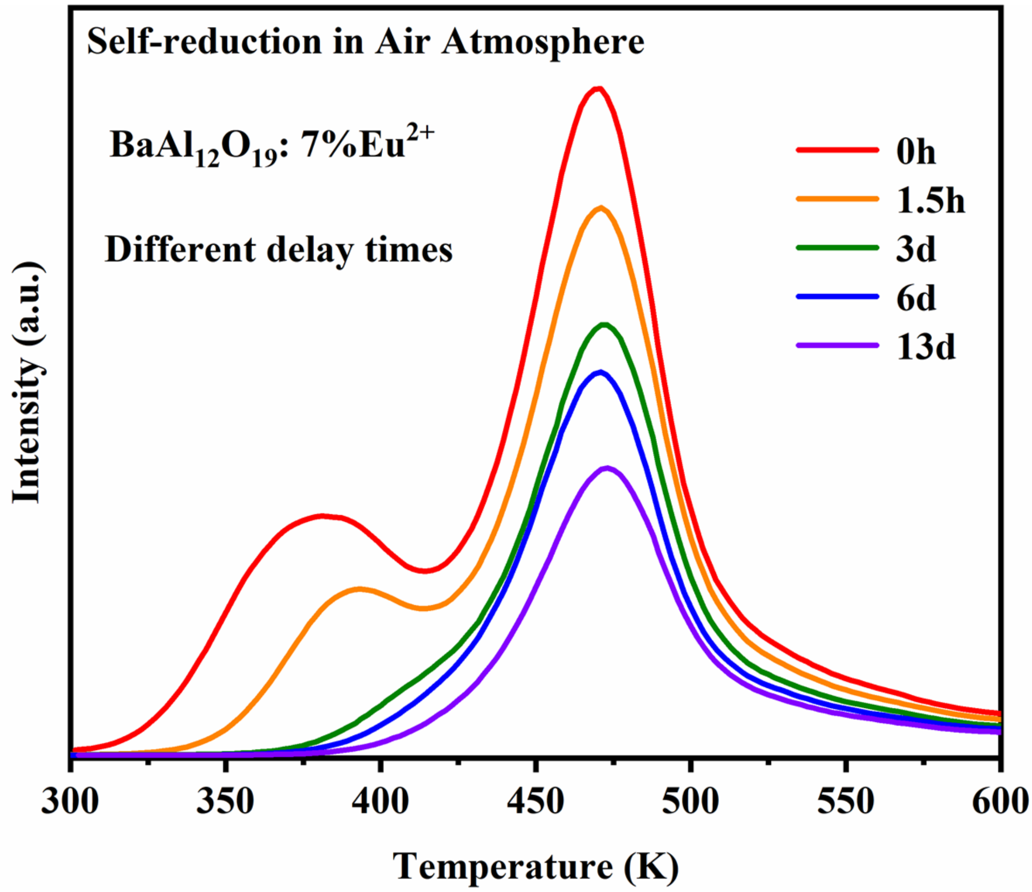


**Figure S3.** TL curves of $BaAl_{12}O_{19}$: 7%$Eu^{2+}$ sample measured at various delay durations after UV light pre-irradiation for 10 minutes. (Self-reduction in air atmosphere)

Based on the Urbach method, the trap depth ($E_t$) can be derived from the location of $T_m$ by using the following empirical expression: [1, 2]

$$E_t = \frac{T_m}{500}$$

$T_m$ is the temperature at the TL peak position.

**Figure S2** shows that the sample is irradiated under a UV lamp for about 7 hours, and the carriers in its traps are saturated. **Figure S3** shows that the deep traps of this sample persisted even after 13 days of exposure to UV light for 10 min. By analyzing the TL curves of $BaAl_{12}O_{19}$: 7%$Eu^{2+}$ samples synthesized in air atmosphere, we proved that the material has the ability to store optical information.

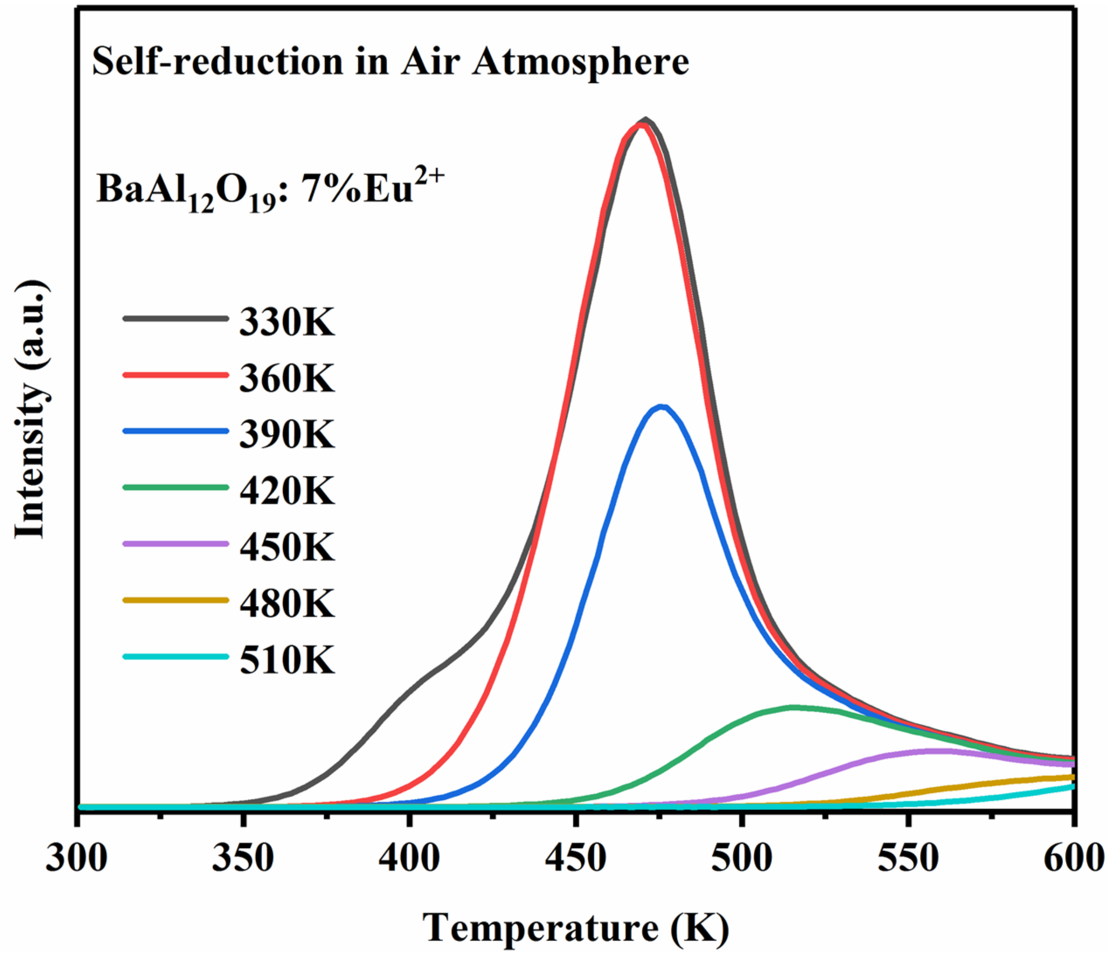


**Figure S4.** Temperature-dependent TL curves of $BaAl_{12}O_{19}$: 7%$Eu^{2+}$ sample with UV light pre-irradiation for 10 minutes for each temperature measurement. (Self-reduction in air atmosphere)

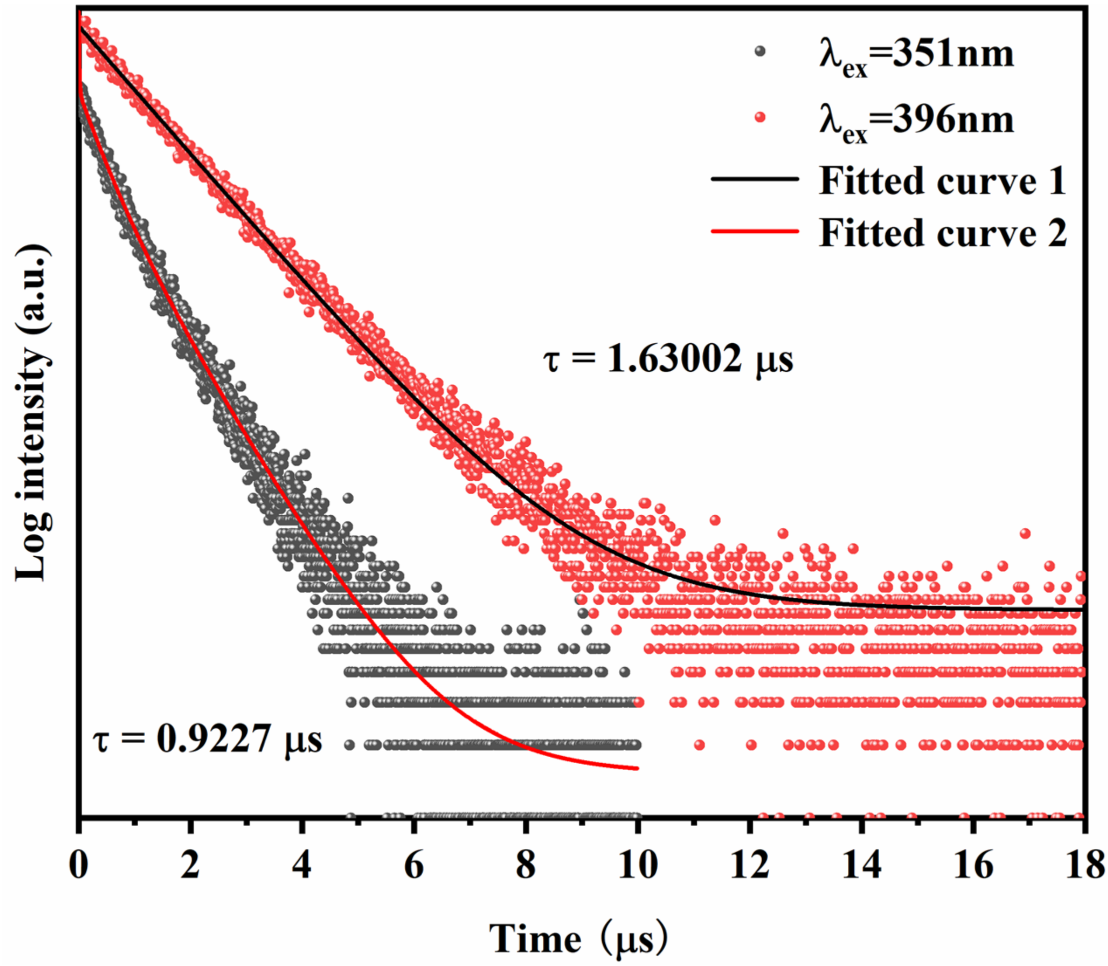


**Figure S5.** The fluorescence decay curves of R-$BaAl_{12}O_{19}$: 7%$Eu^{2+}$ sample measured at different excitation wavelengths. (Reducing atmosphere

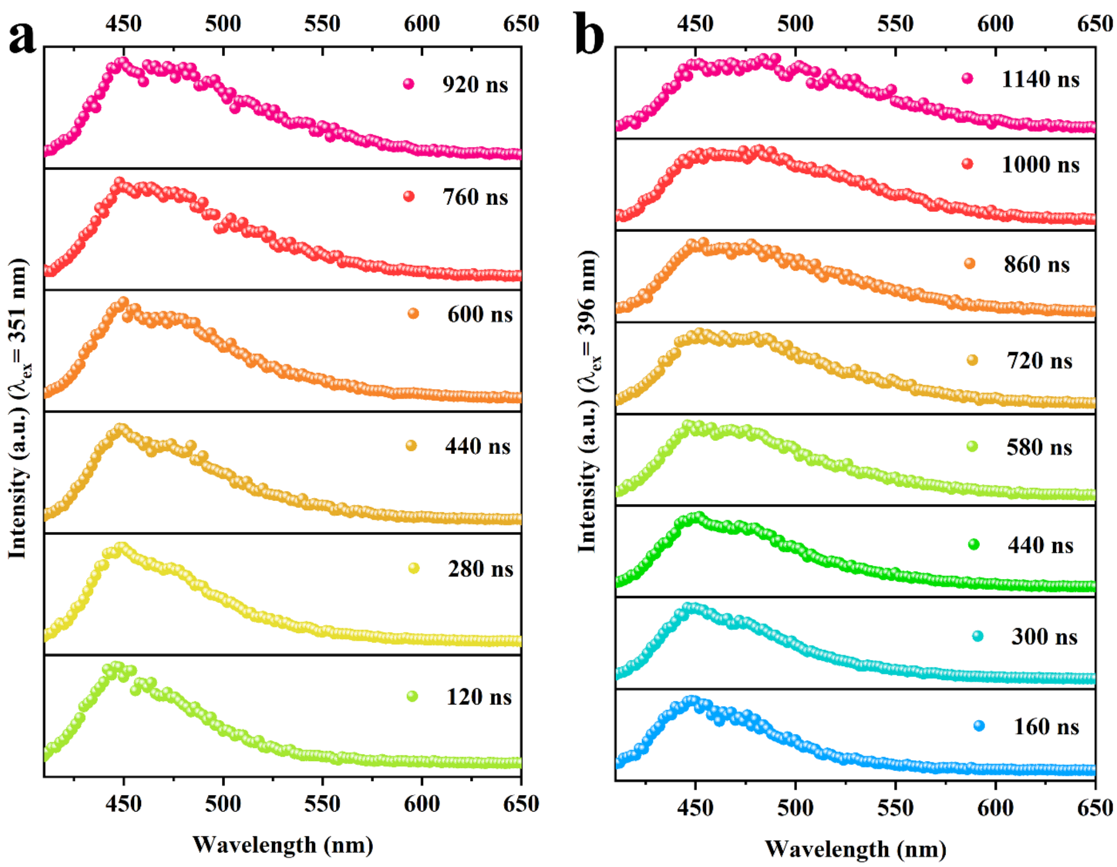


**Figure S6. (a)** TRPL of R-$BaAl_{12}O_{19}$: Eu ($\lambda_{ex}$ = 351 nm), **(b)** TRPL of R-$BaAl_{12}O_{19}$: Eu ($\lambda_{ex}$ = 396 nm).

Time-Resolved Photoluminescence (TRPL) is also a powerful tool for analyzing site occupancy. Therefore, in order to further verify the occupancy of Ba (1)$O_9$ and Ba (2)$O_{10}$ sites of $Eu^{2+}$, we measured the TRPL spectra of R-$BaAl_{12}O_{19}$: $Eu^{2+}$ under excitation at 351 nm, as shown in **Figure S6. (a)**, from this figure, it can be clearly observed that the TRPL spectra show a similar shape to the PL spectra, and the spectra present two emission peaks. It is very important that with the delay of the monitoring time, the relative intensities of the low-energy peak (near 500 nm) and the high-energy peak (near 450 nm) gradually increase, which indicates that there are two luminescent centers in R-$BaAl_{12}O_{19}$: $Eu^{2+}$ and the low-energy peak is attributed to the occupation of Ba (2)$O_{10}$ site by $Eu^{2+}$, the high energy peak is attributed to the occupation of Ba (1)$O_9$ site by $Eu^{2+}$.

In addition, we also measured the TRPL spectra of R-$BaAl_{12}O_{19}$: $Eu^{2+}$ under excitation at 396 nm, as shown in **Figure S6. (b)**, when the monitoring time was delayed from 160 ns to 1140 ns, the shape of the TRPL spectra appeared more obvious than that in

**Figure S6. (a)**, and the relative intensity of the low-energy peak (near 500 nm) and high-energy peak (near 450 nm) is still increasing gradually, and the conclusion is also consistent with **Figure S6. (a)**.

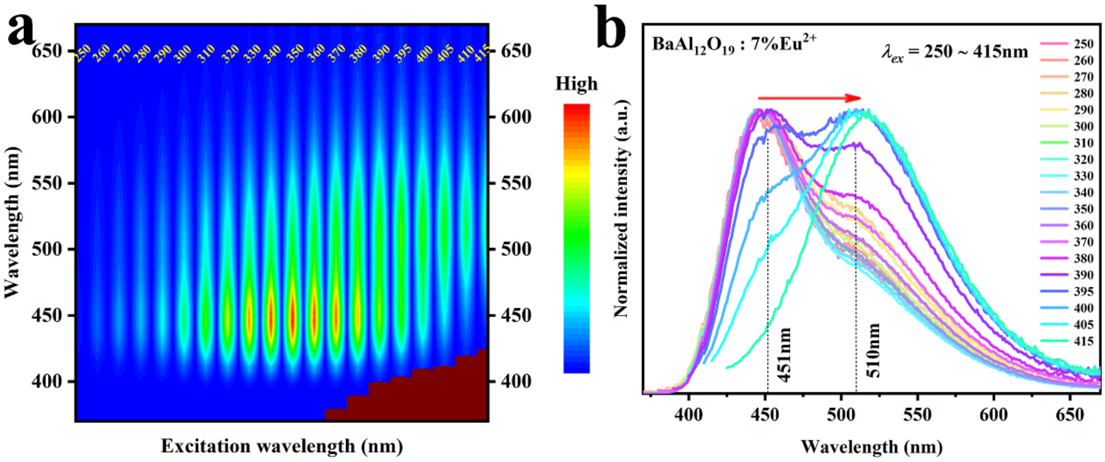


**Figure S7. (a)** 2D contour map of emission spectra measured at different excitation wavelengths ($\lambda_{ex}$ = 250 ~ 415nm), **(b)** Normalized emission spectra of R-$BaAl_{12}O_{19}$: 7%$Eu^{2+}$ sample as a function of different excitation wavelengths. (Reducing atmosphere)

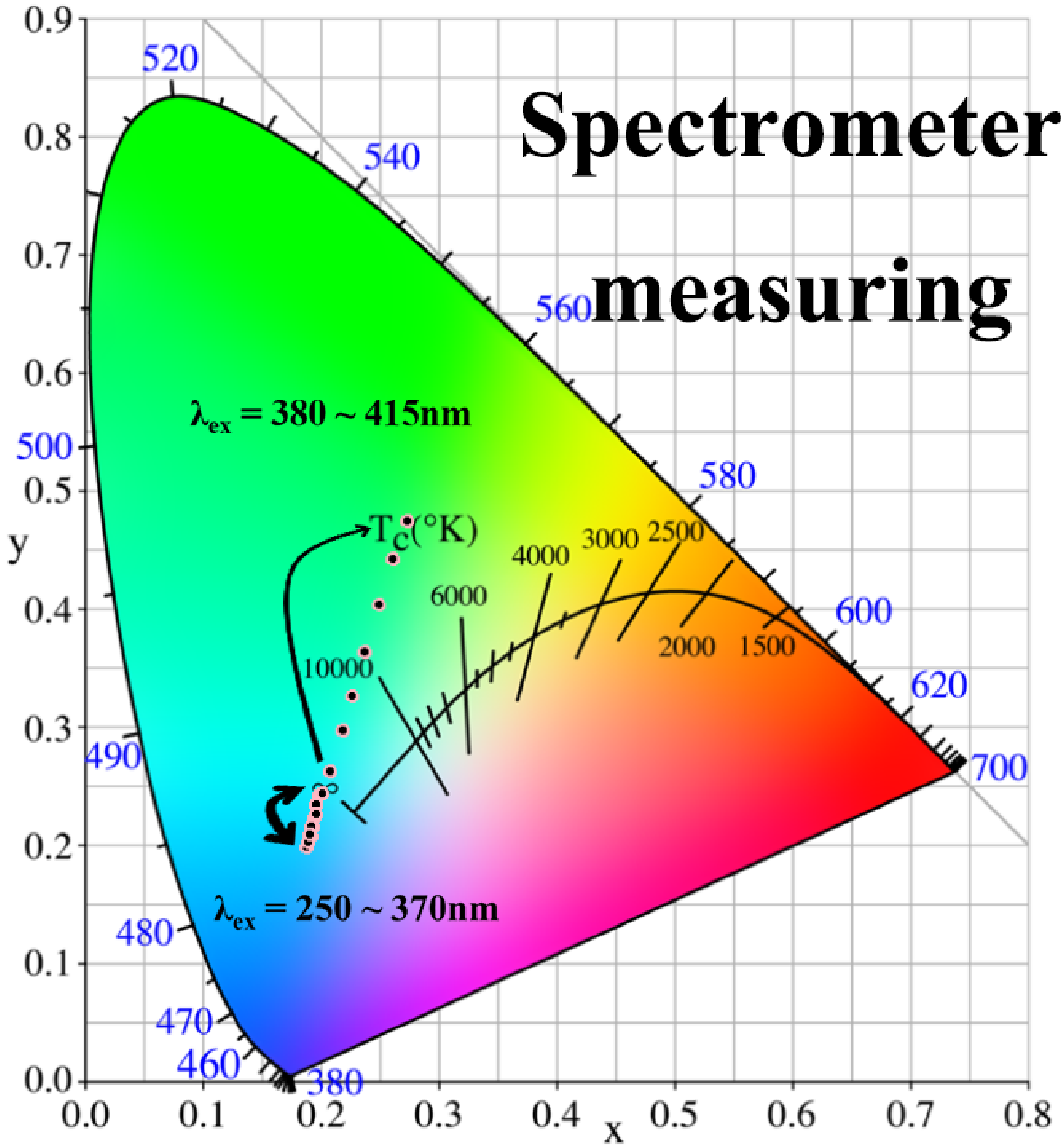


**Figure S8.** Excitation wavelength dependent CIE coordinates of R-$BaAl_{12}O_{19}$: 7%$Eu^{2+}$ sample. (Reducing atmosphere)

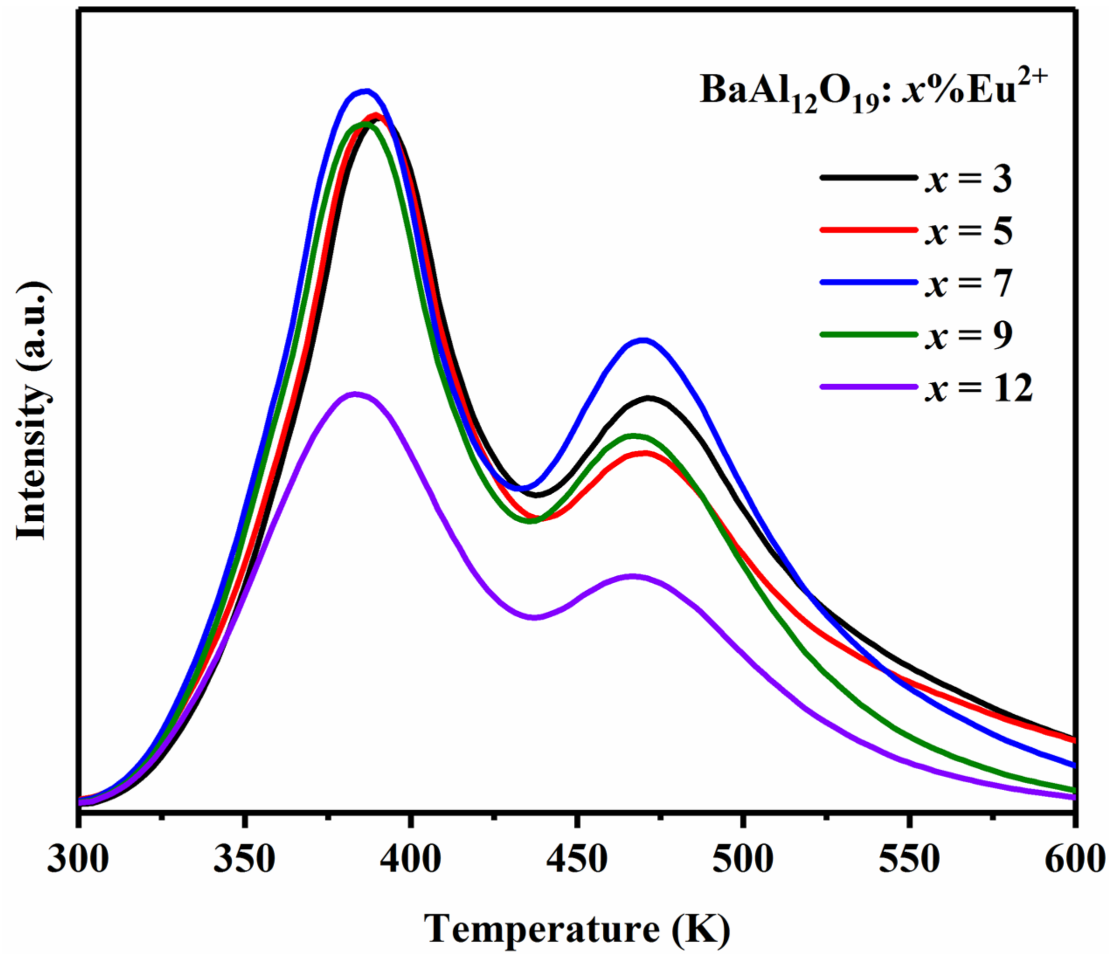


**Figure S9.** TL glow curves of R-$BaAl_{12}O_{19}$: *x*%$Eu^{2+}$ ($3 \leq x \leq 12$) samples with different doping concentrations pre-irradiation with UV light for 10 minutes. (Reducing atmosphere)

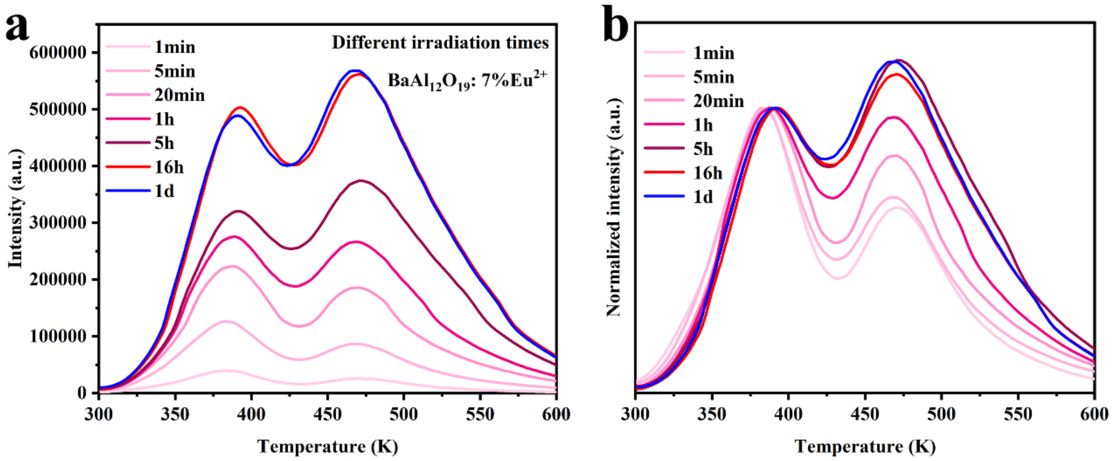


**Figure S10. (a)** Pre-irradiation time dependent TL curves of R-$BaAl_{12}O_{19}$: 7%$Eu^{2+}$; **(b)** Normalized TL curves. (Reducing atmosphere).

When the irradiation time is 16 hours, the TL intensity will reach a saturation state (**Figure S10 (a)**). We normalized the intensity of the shallow traps in **Figure S10 (a)**, and it can be seen from the obtained **Figure S10 (b)** that when the irradiation time exceeds 5 hours, the intensity of the deep traps in the TL curve will be higher than shallow traps. This result indicates that the R-$BaAl_{12}O_{19}$: 7%$Eu^{2+}$ sample can be used as a medium for optical information storage and readout.

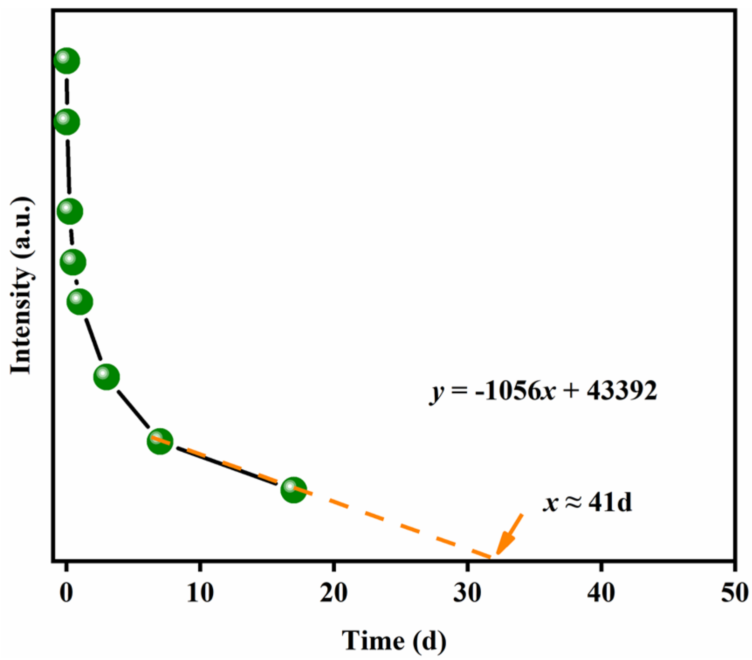


**Figure S11.** In Figure 4b, the deep trap intensities of the TL curves of the R-$BaAl_{12}O_{19}$: 7%$Eu^{2+}$ samples synthesized under a reducing atmosphere were placed for different delay times, and the relationship with different delay times was fitted.

By fitting the relationship between the intensity of the deep traps and the delay time (**Figure S11**), it is known that the stored optical information will disappear after a delay of about 41days.

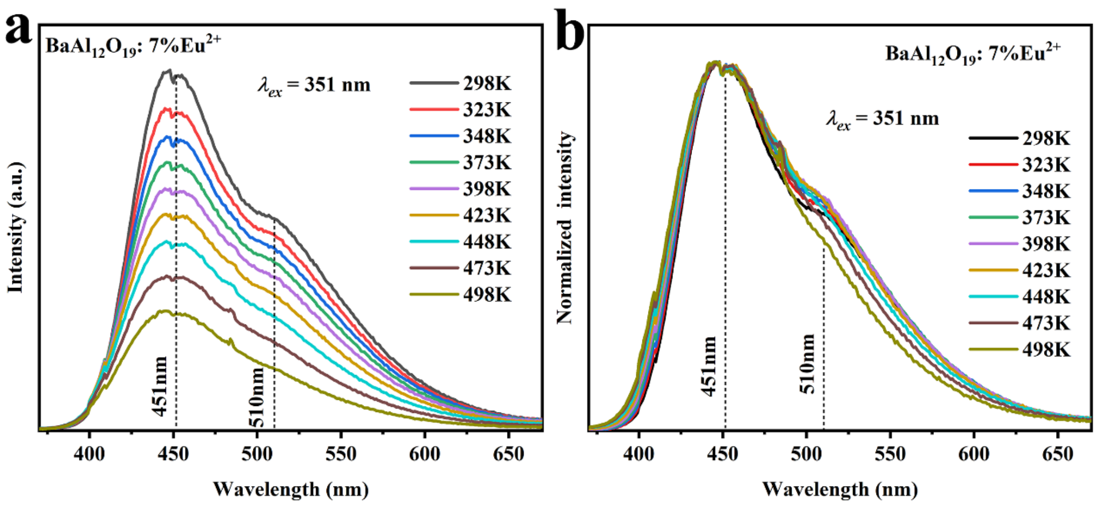


**Figure S12. (a)** Temperature-dependent PL spectra of R-$BaAl_{12}O_{19}$: 7%$Eu^{2+}$. (Reducing atmosphere). **(b)** Normalized spectra of temperature-dependent PL spectra of R-$BaAl_{12}O_{19}$: 7%$Eu^{2+}$. (Reducing atmosphere).

It can be seen that, during the process of increasing the temperature from 298K to 498K, the main peak of PL did not change and was always at 451nm.

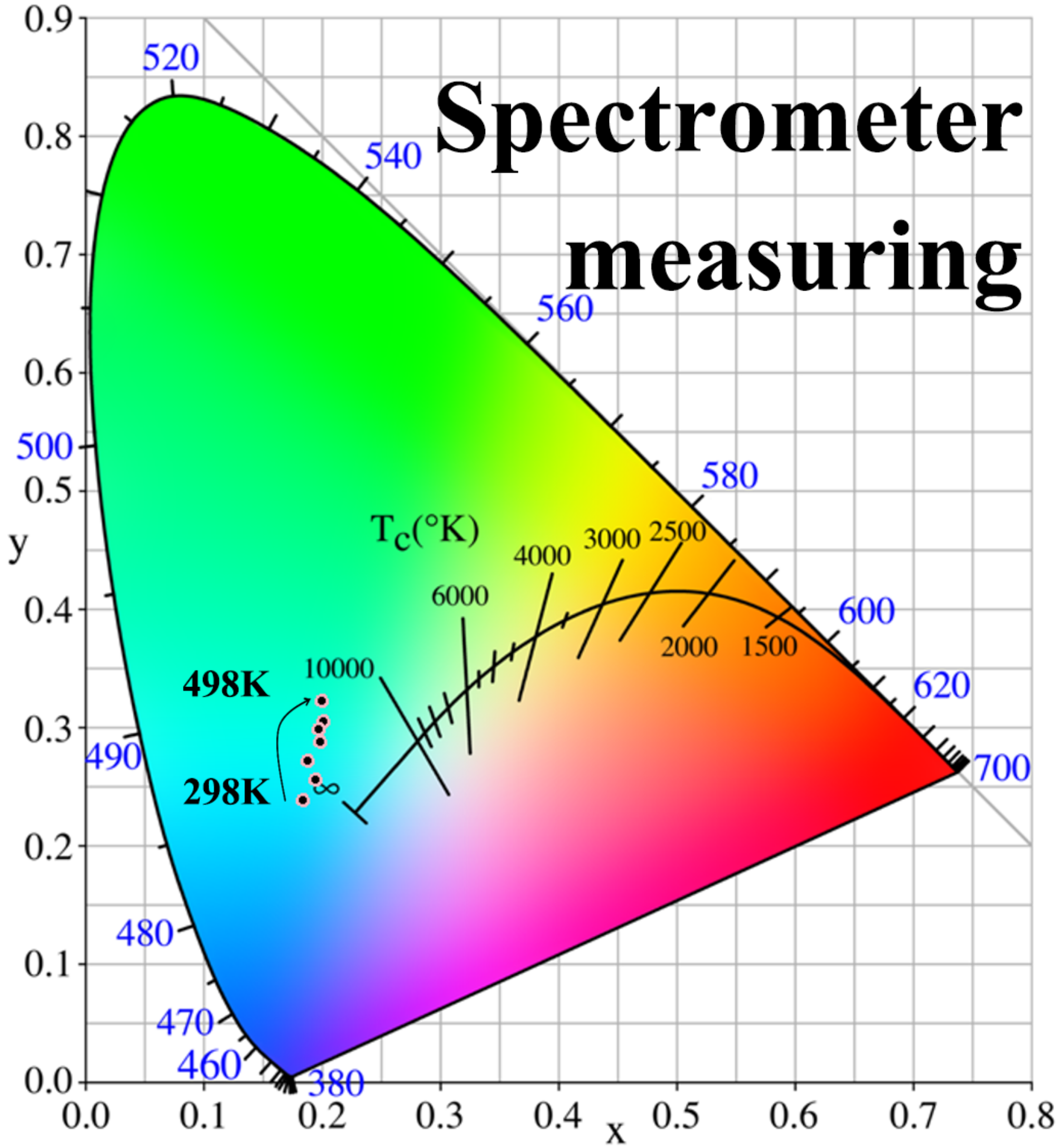


**Figure S13.** CIE coordinates of TSL obtained at different temperature of R-$BaAl_{12}O_{19}$: 7%$Eu^{2+}$ sample. (Reducing atmosphere)

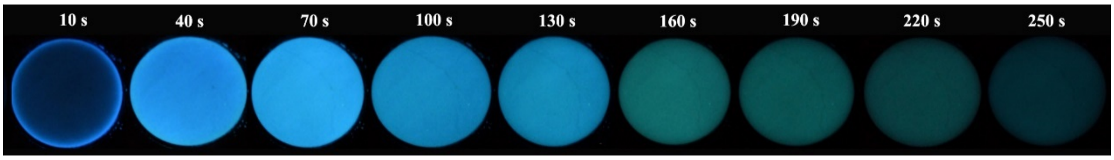


**Figure S14.** TSL images of the R-$BaAl_{12}O_{19}$: 7%$Eu^{2+}$. (Reducing atmosphere)

The $BaAl_{12}O_{19}$: 7%$Eu^{2+}$ sample was pre-irradiated with UV light for 20 minutes, and then placed on a heating table that had been heated to 400 °C. Under thermal stimulation, the sample produced TSL, and a camera was used to record the TSL pictures every 30 seconds. From **Figure S14**, we can see that under the constant temperature stimulation of 400 °C, the stored carriers in the $BaAl_{12}O_{19}$: 7%$Eu^{2+}$ sample are released, and the TSL color changes from blue to cyan over time. The TSL phenomenon disappeared after lasting about 5 minutes.

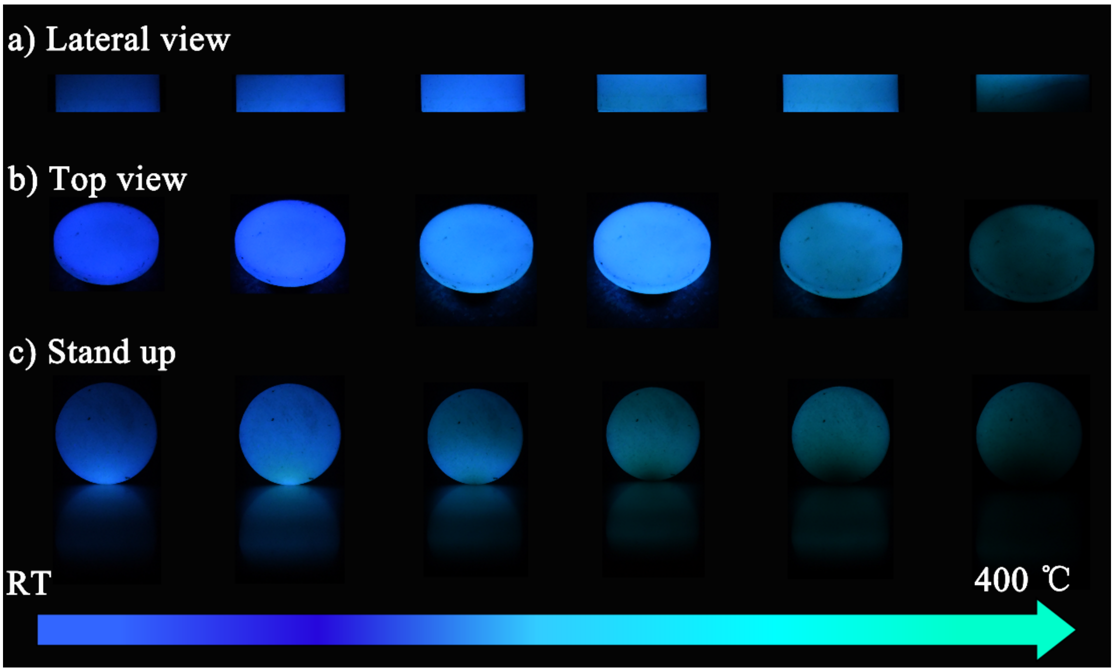


**Figure S15.** TSL images of the R-$BaAl_{12}O_{19}$: 7%$Eu^{2+}$/KBr tablet. (Reducing atmosphere)

The prepared tablets ($BaAl_{12}O_{19}$: 7%$Eu^{2+}$/KBr) were pre-irradiated with UV light for 20 minutes, and then the tablets were placed flat on a heating table at RT. Turn on the heating table and gradually heat up to 400°C. As the temperature gradually increases, the prepared tablets begin to exhibit the TSL phenomenon. Continuously take photos of (**Figure S15(a)**) the side and (**Figure S15(b)**) the top. The TSL phenomenon was recorded. In addition, we also tried to record the TSL phenomenon in the same way by (**Figure S15(c)**) erecting the pre-irradiated tablet on a heating table at room temperature.

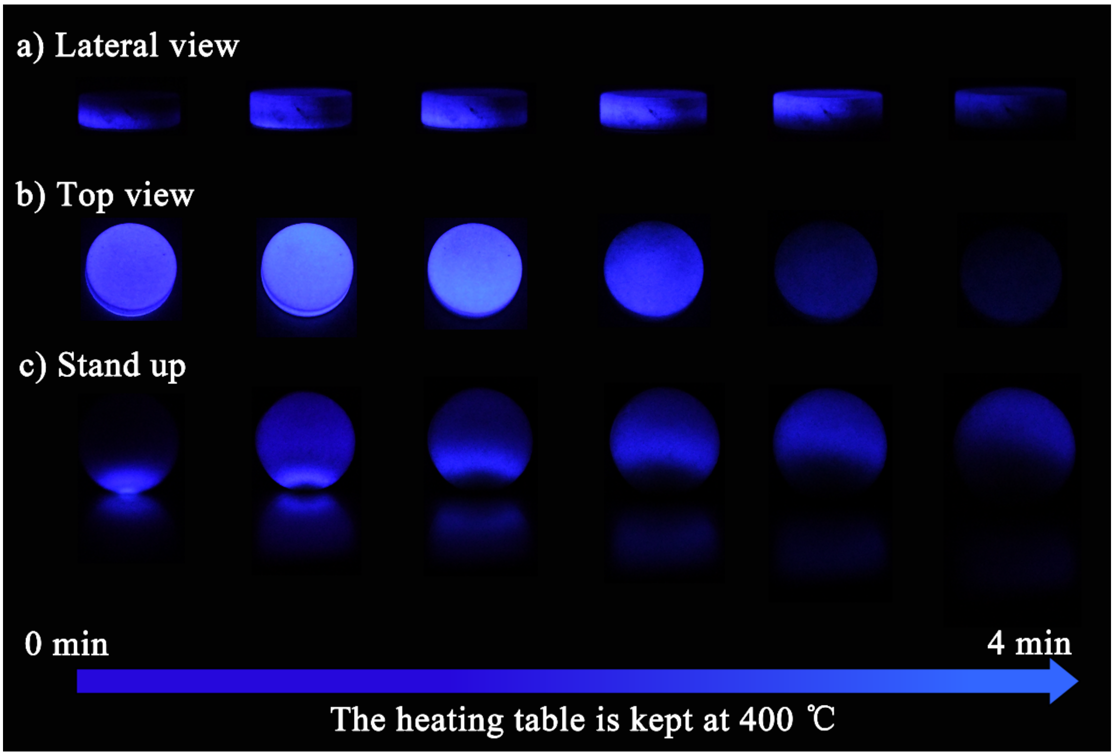

**Figure S16.** TSL images of the $BaAl_{12}O_{19}$: $Eu^{2+}$/KBr tablet. (Self-reduction in air atmosphere)

**Reference**


[1] Z. C. Liu, L. Zhao, X. X. Yang, L. L. Yang, H. Zhang, W. Zeng, X. Yu, J. B. Qiu, X. H. Xu, Long persistent luminescence properties of $NaBaScSi_2O_7$: $Tb^{3+}$ and it's applications above room temperature, *Chem. Eng. J.,* 2020, **401**, 126119.

[2] Z. H. Zhou, X. Wang, X. D. Yi, H. Ming, Z. J. Ma, M. Y. Peng, Rechargeable and sunlight-activated $Sr_3Y_2Ge_3O_{12}$:$Bi^{3+}$ UV–Visible-NIR persistent luminescence material for night-vision signage and optical information storage, *Chem. Eng. J.,* 2021, **421**, 127820.

[3] X. Yu, X. H. Xu, P. H. Yang, Z. W. Yang, Z. G. Song, D. C. Zhou, Z. Y. Yin, Q. Jiao, J. B. Qiu, Photoluminescence properties and the self-reduction process of $CaAl_2Si_2O_8$: Eu phosphor, *Mater. Res. Bull.,* 2012, **47**, 117-120.

[4] J. L. Zhong, L. X. Yu, X. Q. Man, W. Sun, X. Wu, X. F. Jiang, Z. Y. Gao, Q. H. Guo, Y. X. Zou, The self-reduction synthesis and luminescent properties of $Eu^{2+}$/$Eu^{3+}$ activated $BaZr_xSi_3O_{7+2x}$ phosphors with white light emission for white light-emitting diodes, *Luminescence,* 2018, **33**, 1387-1393.

[5] Y. T. Zhu, C. X. Li, D. G. Deng, B. W. Chen, H. Yu, H. Li, L. Wang, C. Y. Shen, X. F. Jing, S. Q. Xu, A high-sensitivity dual-mode optical thermometry based on one-step synthesis of $Mn^{2+}$: $BaAl_{12}O_{19}$–$Mn^{4+}$: $SrAl_{12}O_{19}$ solid solution phosphors, *J. Alloys Compd.,* 2021, **853**, 157262.